

INTEGRATION OF SENTINEL-1A SAR, HYDRO DYNAMIC AND TRAJECTORY MODEL OF OIL SPILL AT BALONGAN COASTAL WATER JAVA SEA, INDONESIA

Muhammad HELMI¹, Agus HARTOKO^{2*}, Hifzhan HUSNA¹
and Mochamad Indra Bayu ARDIANSYAH¹

DOI: 10.21163/GT_2022.171.05

ABSTRACT:

Oil spill is a crucial issue for marine ecosystems, it is necessary to develop such a comprehensive and accurate oil spill detection and mitigation plan for counter measure. Balongan coastal water, Java Sea is an oil loading, unloading and refinery station. The study aims to determine the wide extent area, volume and monsoonal trajectory and volume of the oil spill in Balongan coastal water. The new paradigm of this study is the integration of 58 sets of Sentinel-1A SAR data analysis had resulted to 11 data sets confirmed with oil spill events. Then used as spatial reference, date, tide data and classification of oil spill to develop numeric trajectory model using hydrodynamic GNOME software. The numerical trajectory model for oil spill was running up from day-0 to 10 days or 240 hours period. Sea surface current during transition-1 April to May 2019 range 0.038-0.045 m.s⁻¹, wind speed range 2.53-3.28 m.s⁻¹. Sea surface current during the east monsoon of September 2019 0.191 m.s⁻¹, wind speed 4.33 m.s⁻¹. Sea surface current during transition-2 October to November 2019 range 0.139-0.214 m.s⁻¹, wind speed range 3.16-4.33 m.s⁻¹. Sea surface current during the west monsoon of December 2019 to February 2020 in the range of 0.251-0.369 m.s⁻¹, wind speed range 2.59-4.42 m.s⁻¹. Sea surface current and wind direction in Balongan coastal water Java Sea is predominantly to the northwest direction during the transition-1 April to May 2019 and east season September 2019. Wind and sea surface current during the transition-2 of October to November 2019 and December 2019 – February 2020 is predominantly to the southeast direction. Period of transition-1 April to May 2019 wide of oil spill range 42.80-113.40 km² and volume range 29.95-79.38 barrel of light crude oil. During the east monsoon of September 2019 is the lowest oil spill with wide area of 23.25 km² and smallest oil spill volume of 11.62 barrel of diesel oil. During transition-2 period October to November 2019 wide area range 65.54-78.66 km² volume range 39.07-45.88 barrel of diesel oil and light crude oil. During the west monsoon December 2-19 to February 2020 wide area range 27.08-107.90 km² volume range 13.54-82.37 km² of medium crude oil, light crude oil and diesel oil. Oil spill after 5 days or 120 hours trajectory model, wide area range of 12.10-57.07 km², and most events during the transition-1 and the east monsoon were dispersing out after 10 days or 240 hours. Oil spill trajectory model after 10 days or 240 hours period wide area range 19.98-144.85 km² happened during the transition-2 November to December 2019. Evaporation rate during 10 days trajectory model is in the range of 21.5-56.9 % after 120 hours.

Key-words: Sentinel-1A, SAR, Hydrodynamic, Oil spill, Spatial, Temporal, Trajectory

1. INTRODUCTION

Oil spill is a mixture of oil, hydrocarbon and drilling cuts such as 'oil-based mud' and seawater. Which can harm to the coastal ecosystems, also both direct and indirect economic losses and long-term adverse effects of the above element interactions (Liu *et al.*, 2015).

¹Department of Oceanography, Faculty of Fisheries and Marine Science and Center of Excellent for Science and Technology (PUI), Center for Coastal Disaster Mitigation and Rehabilitation Studie (CoREM), Diponegoro University, Indonesia, muhammadhelmi69@gmail.com, hifzhanhusna98@gmail.com, indrabayuardiansyah04@gmail.com

²Department of Aquatic Resource Management. Faculty of Fisheries and Marine Science. Diponegoro University, Indonesia. *Corresponding author: agushartoko.undip@gmail.com

Oil spill can cause adverse impacts and damage to mangroves, marine invertebrates, seabirds, marine mammals, as well as the composition of microbial communities. Socio-economic impacts can also be evaluated because they disrupt the water quality for aquaculture and coastal tourism. Public health can also be threatened because of the possible impact into the human food chain (Zhang *et al.*, 2019; Kingston 2022). The existing oil spill trajectory simulation is using 2D-hydrodynamic modelling using the General NOAA Operational Modeling Environment (GNOME) considering that the model has its high predictive accuracy. The modelling is based on Lagrangian discrete elements which allow the simulation of oil spill behavior (spots) during the breakdown process which includes dispersion, evaporation, dispersion, and advection (Balogun *et al.*, 2021). Qiao *et al.* (2019) examined the three-dimensional oil spill modeling to simulate and project the short- and long-term trajectories of oil slicks and oil-contaminated water leaking from debris in the Ryukyu Island Chain, Tsushima Strait, on the southern and eastern coasts of Japan. This research used the data of seawater temperature, ocean currents, wind and surface waves using the Lagrangian method which has been successfully applied to produce oil spill trajectory models. Various previous study with the use of 2D-hydrodynamics using GNOME conducted by Heidaria *et al.*, (2019), Naz *et al.*, (2021) and Balogun *et al.*, (2021). In conducting the hydrodynamic modelling using GNOME simulation to determine the trajectory of oil spills and effect of seasonal wind direction in the form of wind rose.

The previous 2D-hydrodynamic modelling study more focused on the trajectory of oil spills, but not yet to the volume of oil spills. To fill in the gaps of the previous research, this study will implement an integrated approach to the use of SAR radar data and hydrodynamic modeling and ultimately the volume of the oil spill. Synthetic Aperture Radar (SAR) satellite is a versatile sensor that can be operated in any weather and time of day or night (Fletcher, 2012; Josaphat and Nobuyoshi, 2016; Rajendran *et al.*, 2021). SAR data is commonly used to monitor oil spills at sea where the microwave beam is emitted by the sensor and the received signal is reflected into the backscatter object features (Fan *et al.*, 2015). In this case, the best method is using the digital number or spectral signature by means of the threshold spectral value analysis to detect the dark object as the oil spill, and spatial-temporal analysis approach (Cantona *et al.*, 2019; Chaturvedi *et al.*, 2020; Fan *et al.*, 2015; Li *et al.*, 2019). Balongan coastal water, Indramayu Regency Java Sea is extensively used for oil refinery, and distribution processed crude oil activities and gas companies. Crude oil supply activities to the Balongan refinery generally use oil tankers originating from Riau province, Sumatera. The oil tankers or carrier ships are moored at the mooring facilities, namely Single Point Mooring (SPM) with the Jetty Cargo facility. Through SPM, crude oil carried by transport ships is unloaded and transported to the Balongan oil refinery. This makes Balongan coastal water becomes a highly oil spill risk coastal water (Sinurat *et al.*, 2016). A comprehensive study is needed to determine the distribution of the oil spill trajectory to determine further policies in dealing with especially to estimate how and where the oil can spread (Heidaria *et al.*, 2019). The analysis represents the observed natural phenomena in the spatial and temporal dimensions where the data considered the spatial dependencies between the observed areas and its correlation of one or several time periods image data.

The new paradigm in study is aimed to apply integration of processed Sentinel-1A SAR to determine the initial, actual and wide area of the oil spill and 10 days trajectory modelling or spatial distribution pattern after the initial oil spills and ultimately analysis the volume of oil spills using GNOME method for four monsoons period namely transition-1 (March-April-May), the east monsoon (June-July-August, September), transition-2 (October-November) and west monsoon (December-January-February). The result of study can provide comprehensive data and information on oil spills to the oil companies and operators, environmentalists, and researchers in carrying out mitigation efforts and handling strategies. The spatial numerical model in this study can be adapted and implemented in other areas where oil spills frequently occur.

2. STUDY AREA

The study area is located in Balongan coastal water, Indramayu Regency Java sea, with coordinates of 6°14'2.72" - 6°28'50.96" South Latitude and 108°20'38.84" - 108°35'40.24" East Longitude (**Fig. 1**). The field study was conducted for one year from April 2019 to April 2020.

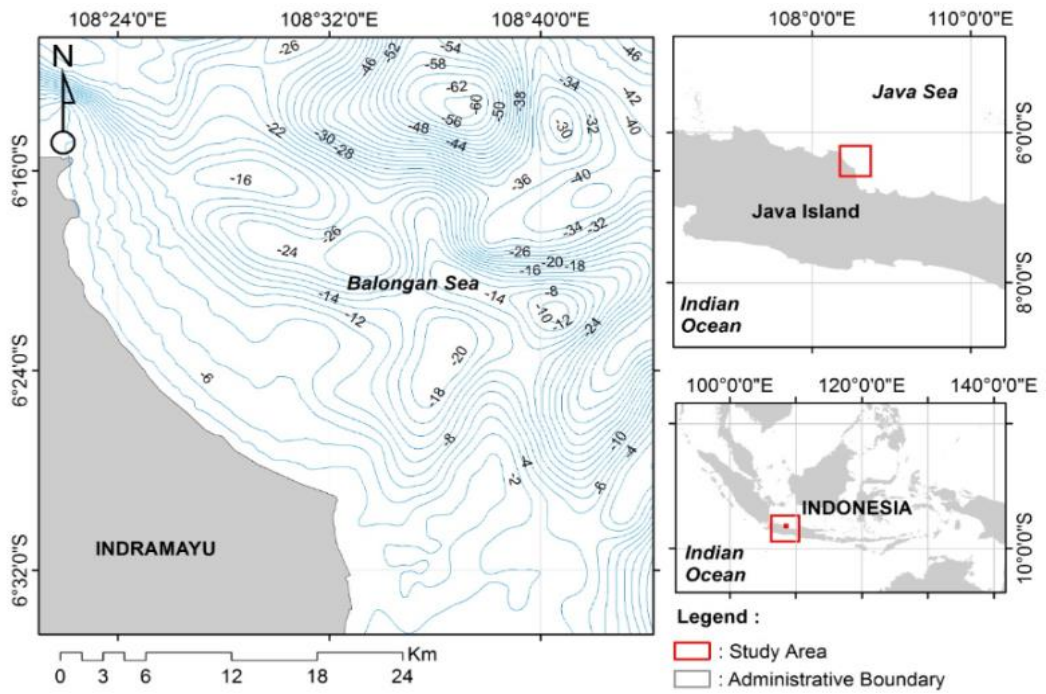


Fig. 1. Map of the study area and bathymetry.

3. DATA AND METHODS

3.1. Data

3.1.1. Wind and Current Data

The horizontal wind direction and wind speed data was obtained from the European Centre for Medium Range Weather Forecasts (ECMWF-<https://www.ecmwf.int>) and represent for 12-months period, starting from April 2019 – March 2020. The obtained wind data was then processed into the components of wind speed of u-component and v-component. After obtaining the direction and total wind speed, the data was displayed in the form of wind rose using WRPlot software. Data of sea surface current was collected from the Hybrid-Coordinate Ocean Model (HYCOM - <https://www.hycom.org>) for one year period. The initial current data was firstly arranged using Microsoft Excel software by selecting the data collection time, coordinates, depth, u-component and v-component. The work was continued using GIS data processing application for the interpretation of the vector direction and velocity of the sea surface current. To produce the total current speed or velocity and direction, the u and v data were compiled and grouped using Ms. Excel. The processed wind data was then used as input data in the modelling of sea surface current speed and direction, and ultimately used for the oil spills hydrodynamic modell using GNOME software to produce the oil spill trajectory modell.

3.1.2. Oil Properties

Oil properties served was used as input for the model for the distribution of oil spills (**Table 1**). The data was in the form of oil, which was distributed through SPM (Single Point Mooring) and Loading Jetties of the state owned PT. Pertamina RU VI Balongan oil refinery. The data on oil loading and unloading activities at Balongan coastal water is used to build the spatial model and assist in analysing the results of oil spill detection. This data was obtained from the oil and gas loading and unloading schedule from PT. Pertamina RU VI Balongan. The data of ship coordinates, ship loading capacity and ship sailing time were used in analysing the type and source of the oil spill.

Table 1.
Oil Properties (Sun *et al.* 2016; Yu. *et al.*, 2018)

Oil Properties	Diesel	Light Crude Oil	Medium Crude Oil
API gravity (deg)	44	31	26
Molecular average weight	194	199	262
Saturation (±1 wt %)	84	71	52
Aromatic (±1 wt %)	12	15	27
Resins (±1 wt %)	4	14	21
n-C7 Asphaltene stability	-	<i>stable</i>	<i>stable</i>
Wax Appearance	18	27	25
Temperature (±1 °C)			
Wax content (wt %)	-	3.1	2.1
SARA analysis at 65 °C.			

3.2. Oil Spill Spatial Distribution

Sentinel-1A SAR is a dual-polarization image data with specifications VV (vertical transmit and vertical receive) and VH (vertical transmit and horizontal receive) Level-1 Ground Range Detected (GRD) obtained from Copernicus Open Access Hub (<https://scihub.copernicus.eu/>). This data represent the period of April 2019 to March 2020, was processed using the SNAP 6.0 application with image correction stages which included geometric, radiometric, and speckle filtering (noise correction). Oil spill detection was carried out using the adaptive threshold method. This method processed dark objects, which are an indication of an oil spill, using the Oil Spill Detection Tool, which is part of the Ocean Application in the SNAP application (Li, 2019). The spatial Sentinel-1A SAR image data was first geometrically corrected to the World Geodetic System, namely WGS 1984 (Hartoko *et.al*, 2016; Hartoko *et.al*, 2019; Fitriyanto *et al.*, 2019). The process of detecting dark objects, which is an indication of an oil spill, used the adaptive threshold method on the Oil Spill Detection tool. If the maximum intensity value is below the average plus a predetermined standard deviation, it can be used to set an adaptive threshold. This limit is used to avoid oil spill detection errors (false negative). After the value was analysed, it would be tested using a quartic function and a negative exponential function as in the equation 1 and 2 below:

$$Y = -6.3401 \times 106X_4 + 0.00073027X_3 - 0.029919X_2 + 0.50015X - 2.6381 \tag{1}$$

$$Y = 7.4199 e^{-0.18212X} \tag{2}$$

where X is the value of the original pixel

Y is the value of the dark pixel value representing for the oil spill object.

The use of these functions would result several referred areas that were originally suspected of being an oil spill zone but are actually negative because these areas are not included in the threshold criteria (Mera *et al.*, 2012; Cantorna, 2019; Chaturvedi *et.al*, 2020).

3.3. Oil Spill Volume

The detection of an oil spill that has been carried out in an interpretation of the dark spot spectrally detected as an oil spill area from the Sentinel-1A SAR data. The data interpretation stage was carried out over a period of 12 months, which was in April 2019 - March 2020. The image was processed using the SNAP application and then it produced a map of the oil spill for each month. Total of 11 image detected with oil spill were obtained from total of 58 processed images. These results represents for the temporal and spatial of oil spill in area of Balongan coastal water. The classification of oil types was determined based on the plot profile value of each pixel in the image. By integrating it with the loading and unloading schedule of ships at Balongan coastal water, the type of oil spill could be determined from PT PERTAMINA Balongan. This thickness value would imply to the classification the oil spill as in **Table 2**. Using the oil type and thickness and the wide extent of

the oil spill could determine the total volume of oil spill. Each image detected with oil spill through Sentinel image processing integrated with classification of oil spill. The volume data was important because it was needed as input data in hydrodynamic modelling of oil spill trajectory.

Table 2.
Classification of oil spill thickness according to Sun *et al.* (2016).

Plot Value (dB)	Thickness (μm)	Oil Type
-15 – (-20)	≤ 50	Diesel
-20 – (-25)	50-200	Light Crude Oil
-25 – (-30)	200-1000	Medium Crude Oil

3.4. Oil Spill Trajectory Using Hydrodynamic Numerical Model

Oil spill numeric spatial modelling was generally built using the GNOME application with the TxBLEND hydrodynamic model. This model uses the sea surface current data from the Hybrid-Coordinate Ocean Model (HYCOM) and wind data from the European Centre for Medium Range Weather Forecasts (ECMWF). The process was continued with the oil spill modelling by entering the oil properties and oil spill volume obtained from the spatial model image analysis for the period April 2019 to March 2020 that had been carried out previously. Sea surface current and oil spill model simulations were carried out for 48 hours (2 days), 96 hours (4 days), 144 hours (6 days), 192 hours (8 days) and 240 hours (10 days). Sea surface current modelling produced the \mathbf{u} -velocity and \mathbf{v} -velocity. The model is a representation of state, object, and event of the oil spill. The representation must be realized in a simple form, by eliminating or minimizing complex variables that are not directly related to the model (Susanti *et al.*, 2019).

Processing the TxBLEND model in GNOME applied the continuity equation, momentum equation and diffusion equation to solve water transport and circulation patterns. The following equations were used to built the spatial numerical model on the trajectory of oil spills in the seawater:

$$\frac{\partial^2 \xi}{\partial t^2} + G \frac{\partial \xi}{\partial t} - \nabla \cdot \left\{ \nabla \cdot (H\vec{V}\vec{V}) + gH\nabla\xi + \frac{gH^2}{2\rho} \nabla\rho + f \times H\vec{V} - HA \right\} + (G - \tau)\nabla \cdot (H\vec{V}) - H\vec{V} \cdot \nabla\tau = G \cdot (r - e) \quad (3)$$

$$\frac{\partial q_i}{\partial t} + \frac{\partial u q_i}{\partial x_i} + \frac{\partial v q_i}{\partial x_i} + gH \frac{\partial \xi}{\partial x_i} + \tau q_i = r_i \quad (4)$$

$$\frac{\partial C}{\partial t} + u \frac{\partial C}{\partial x} + v \frac{\partial C}{\partial y} - \frac{\partial}{\partial x} \left(D_x \frac{\partial C}{\partial x} \right) - \frac{\partial}{\partial y} \left(D_x \frac{\partial C}{\partial y} \right) = s \quad (5)$$

where ξ defines the water level elevation,

τ is the basic friction,

r_i is the wind stress and the Coriolis parameter,

s is the substance concentration C ,

G is the law of continuity.

The sea surface current divergence was calculated from the surface current data (Nordam *et al.*, 2019; Wirasatriya *et al.*, 2020). The spatial modelling of the oil spill trajectory was analysed based on the numerical transformation of current and tidal data (Hartoko *et al.*, 2016; Hartoko *et al.*, 2019). Oil spill modelling is generally done using GNOME software with eularian-lagrangian hydrodynamic model. This equation approach is a simulation involving large and small particles in the sea surface water and examining the mass and momentum of the spilled oil (Remyalekhsmi and Hedge, 2013). This modelling used the data base maps of the Global Custom Maps Generator on NOAA, surface current data of the Hybrid-Coordinate Ocean Model (HYCOM) and wind data of the Global Forecast System (GFS). Then proceed with oil spill modelling by inputting the oil properties and oil spill volume obtained from the analysis for the period April 2019 to April 2020 that was carried out previously.

The following formula of Eulerian-Lagrangian particle tracking method, where L defines as the initial position of the particle at $t_0 + \Delta t$, L_0 is the position of the particle at t_0 , and V_t is the speed of movement of the oil particles (Yang *et al.*, 2013).

$$L = L_0 + \int_{t_0}^{t_0 + \Delta t} V_t(t_0, y(t_0), t_0) dt \tag{6}$$

The particle velocity movement method was applied as follows, where V_t is the current speed at t , V_w is the wind speed at t and αV_w is a linear current driven by the wind carried out by the GNOME model (Yang *et al.*, 2013).

$$V = V_t + \alpha V_w \tag{7}$$

3.5. Oil Volume Estimation After Degradation and Evaporation

The estimated volume of an oil spill could be determined using oil property data (oil characteristic) and wind data, both are processed using the ADIOS 2 (Automated Data Inquiry for Oil Spills) application. Data of oil volume were obtained with integration of oil type and thickness, wind data, current data and wide area. Then the data became input data that was simulated to determine the volume of oil spills from the first day the oil spilled into the waters until the next 5 days. The volume of the oil spill was influenced by salinity, SST, density, wind, waves, and surface currents. These factors will affect the volume of oil which experience the process of dispersion, evaporation, emulsification, spreading, benzene contamination, sinking to the bottom of the water, leakage rate, heat burning due to atmospheric temperature. To determine the evaporation rate of an ADIOS 2 spill, the Pseudo Component (PC) evaporation model was used, with the equation used in the model as follows:

$$\left(\frac{dV}{dt}\right)_j \propto \frac{U^3 V (P_v v f_m)_j}{d} \tag{8}$$

where j determines a certain PC, f_m is the variable molar fraction of the pseudo component, V is the volume of oil, U is the wind speed, and d is the thickness. The relative molar volume is v (Lehr *et al.*, 2002).

4. RESULTS

4.1. Wide Area and Volume of Oil Spill

Total of 58 sets processed Sentinel-1A SAR image data had been analyzed representing the period of April 2019 to March 2020, had resulted to 11 images indicates with oil spill (**Table 3, Figures 2, 3, 4 and 5**). These results represent for the temporal and spatial of oil spill in area of Balongan coastal water. The classification of oil types was determined based on the plot profile cluster of pixel value of each 11 image. The dark spots spectral value detected with oil spill found during the transition-1 in Sentinel-1A SAR data recorded on April 8, 2019 wide area of oil spill is 88.30 km² volume 61.81 barrel. Sentinel-1A SAR image data of April 16, 2019 with wide area of 113.40 km² volume 79.38 barrel, data of May 26, 2019 with wide area of 42.80 km² volume 29.95 barrel all with category of light crude oil. The category of diesel oil spill were found in Sentinel-1A SAR data during the east monsoon September 11, 2019 with wide area of 23.25 km² and volume 11.62 barrel. Sentinel-1A SAR data during the transition-2 of October 13, 2019 wide area of 78.66 km² volume 39.33 barrel and Sentinel-1A SAR data in November 10, 2019 wide area of 78.13 km² volume 39.07 barrel of diesel oil category and data of November 18, 2019 wide area 65.54 volume 45.88 barrel of light crude oil. The Sentinel-1A SAR image data during the west monsoon of December 12, 2019, was recorded with category of medium crude oil spill with wide area of 91.52 km² volume 82.37 barrel. Data of December 16, 2019 wide area 107.90 km² volume 75.53 barrel. Data in January 9, 2020 wide area 56.70 km² volume 28.35 barrel and data in February 14, 2020 wide area of 27.08 km² volume 13.54 barrel.

Table 3.
The date, season, wide area and volume of oil spill based on Sentinel-1A SAR data.

No	Date Detected	Monsoon	Wide Area Detected (km ²)	Volume Detected (barrel)	Oil Type Detected
1	08/04/2019	Transt-1	88.30	61.81	Light crude oil
2	16/04/2019	Transt-1	113.40	79.38	Light crude oil
3	26/05/2019	Transt-1	42.80	29.95	Light crude oil
4	11/09/2019	East monsoon	23.25	11.62	Diesel oil
5	13/10/2019	Transt-2	78.66	39.33	Diesel oil
6	10/11/2019	Transt-2	78.13	39.07	Diesel oil
7	18/11/2018	Transt-2	65.54	45.88	Light crude oil
8	12/12/2019	West monsoon	91.52	82.37	Medium crude oil
9	16/12/2019	West monsoon	107.90	75.53	Light crude oil
10	09/01/2020	West monsoon	56.70	28.35	Diesel oil
11	14/02/2020	West monsoon	27.08	13.54	Diesel oil

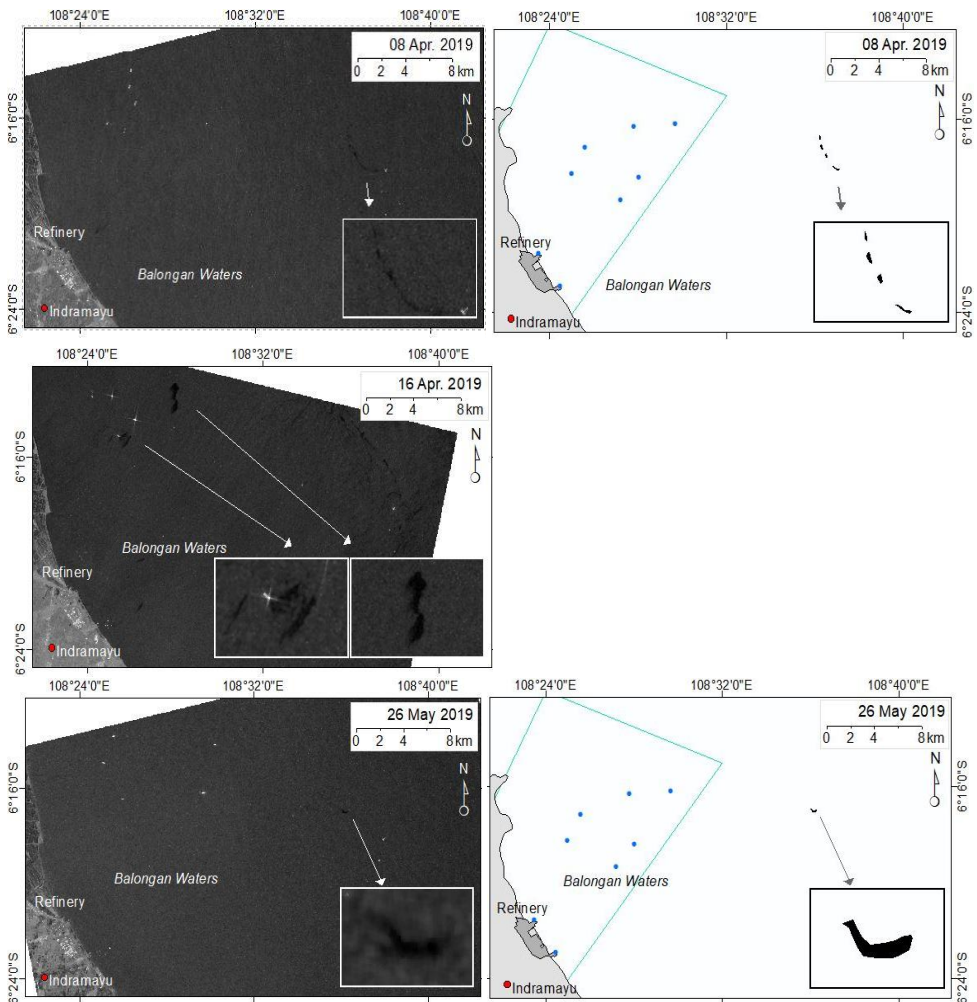


Fig. 2. Oil Spill Analysis of Sentinel-1A SAR Transition-1 April-May 2019.

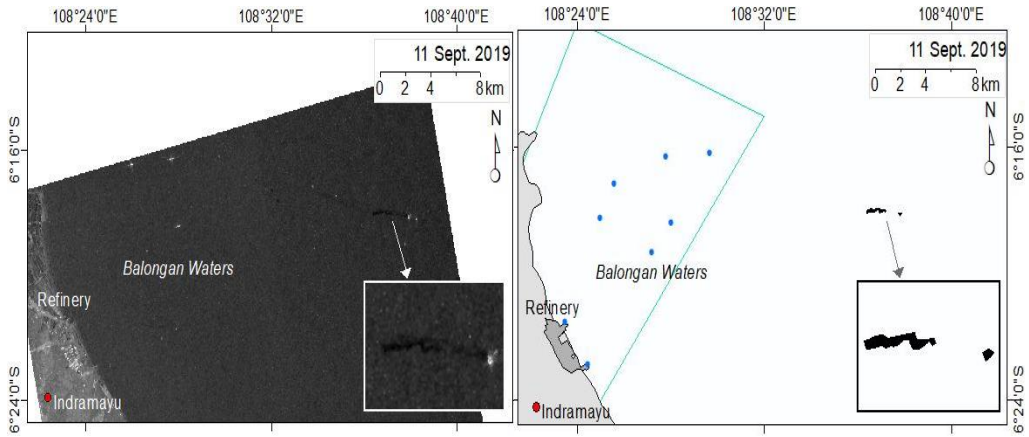


Fig. 3. Oil Spill Analysis of Sentinel-1A SAR East Monsoon September 2019.

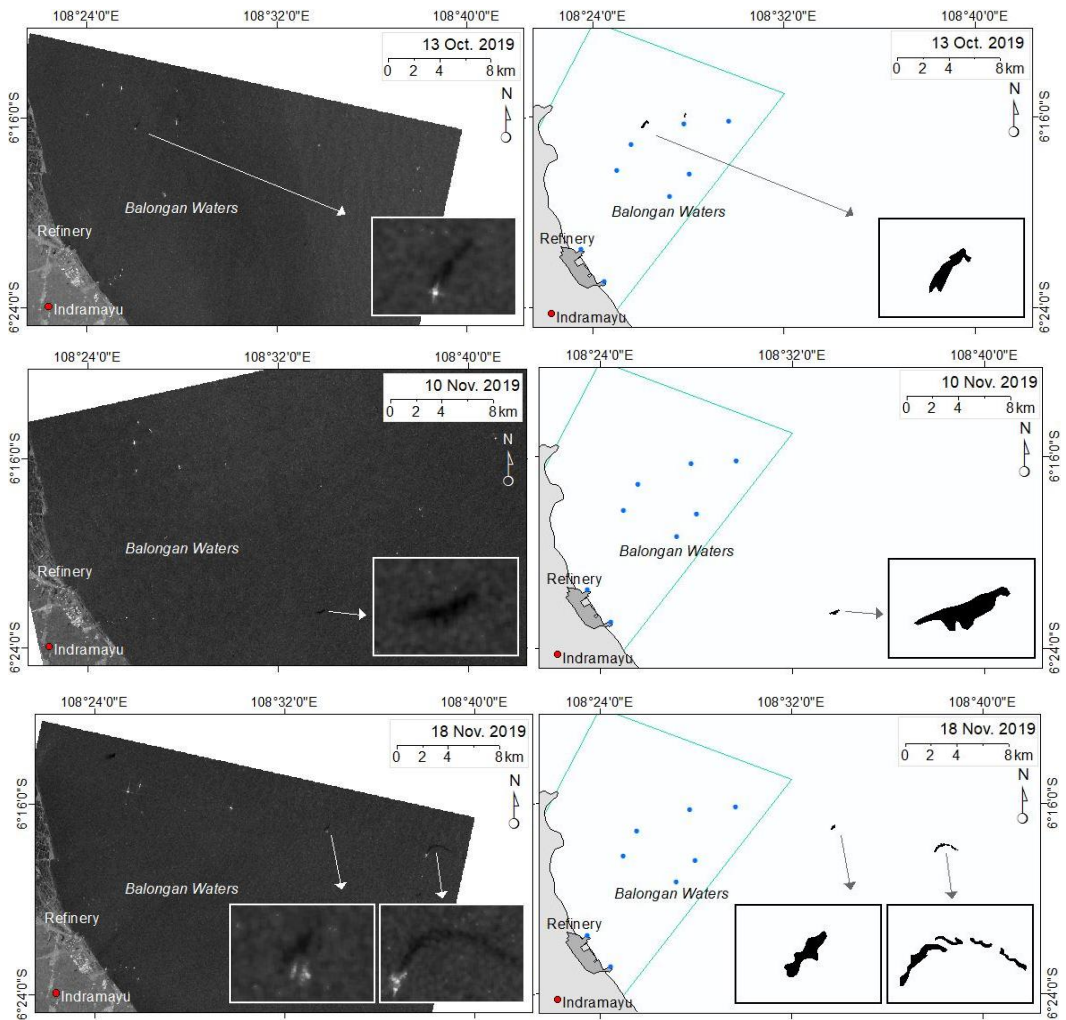


Fig. 4. Oil Spills Analysis of Sentinel-1A SAR During Transition-2 October – November 2019.

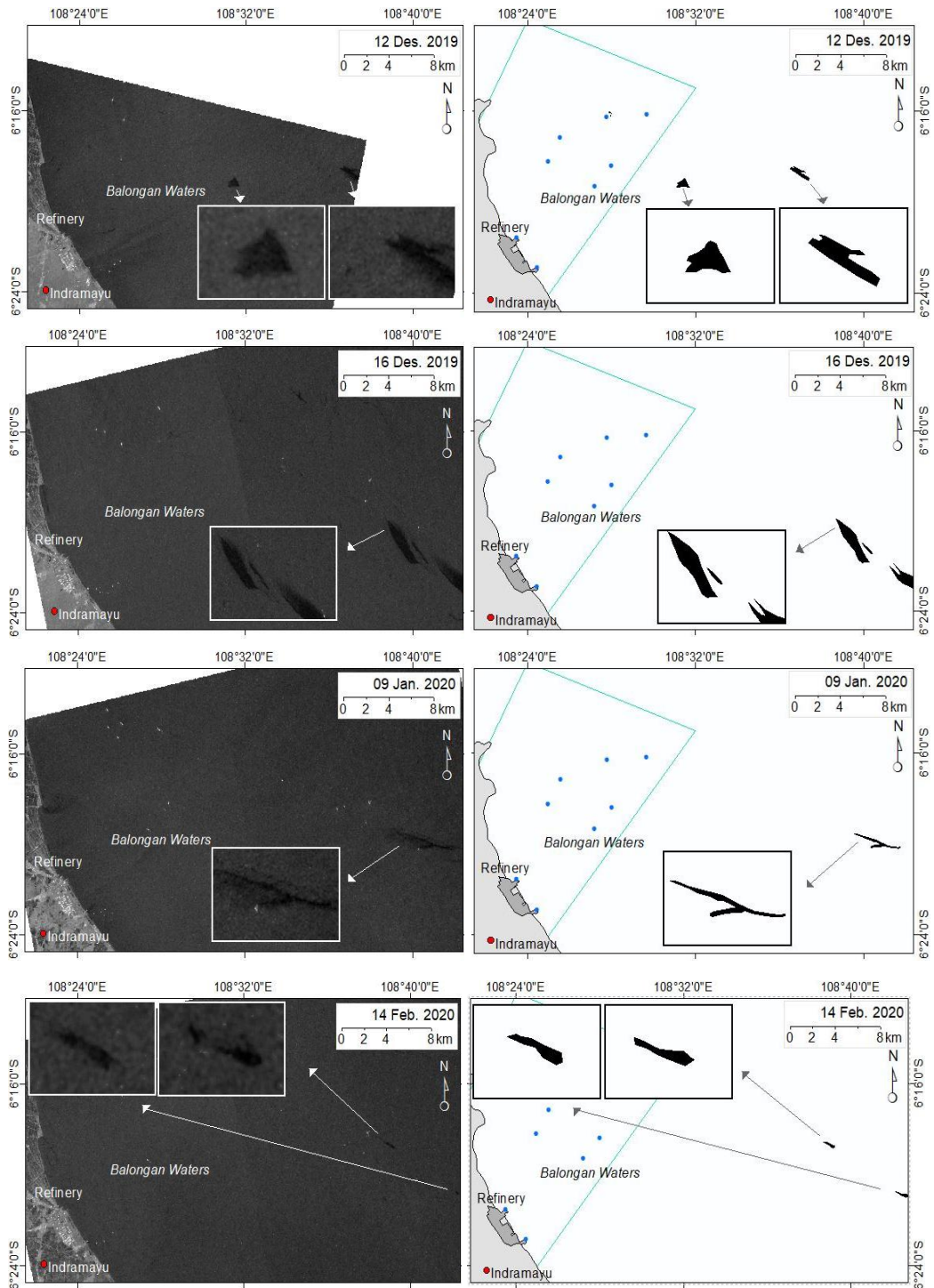


Fig. 5. Oil Spills Analysis of Sentinel-1A SAR During West Monsoon December 2019, January-February 2020.

The category of oil spill which are determined based on the spectral value at each oil spill plot profile, will indicate that the smaller the spectral value was indicator as the thicker the layer of oil spill in seawater. The thicker of the oil spill layer in seawater was assumed as the thicker oil spill

viscosity, which classified as a medium crude oil. Likewise, when the spectral value of the dark spot profile detected is higher spectral value then will be categorized as oil spill with a lower viscosity, which in this case include the category of diesel oil. Meanwhile, when the spectral value is in between of the two-plot profile value is classified as the light crude oil, refer to American Petroleum Institute (API) has the gravity value of 30 - 39.9. The medium crude oil class has API Gravity value of 22 - 29.9 and diesel classified to super-light crude oil with API more than 40 (Sauz *et al.*, 2018).

4.2. Wind and Sea Surface Current Speed and Directions

The numerical wind data obtained from European Centre for Medium Range Weather Forecasts is specifically represent the study area at Balongan coastal water only. Predominant wind direction during the transition-1 of April and May 2019 is from the east with speed range of 2.10– 5.70 m.s⁻¹ (Fig. 6). Predominant wind direction during the east monsoon is southeast direction with speed range of 3.60-5.70 m.s⁻¹ (Fig. 7). Predominant wind direction during the transition-2 of October-November 2019 is southeast direction with speed range of 2.10-5.70 m.s⁻¹ (Fig. 8). Predominant wind direction during the west monsoon December 2019-February 2020 is from the west with wind speed range of 2.10-5.70 m.s⁻¹.

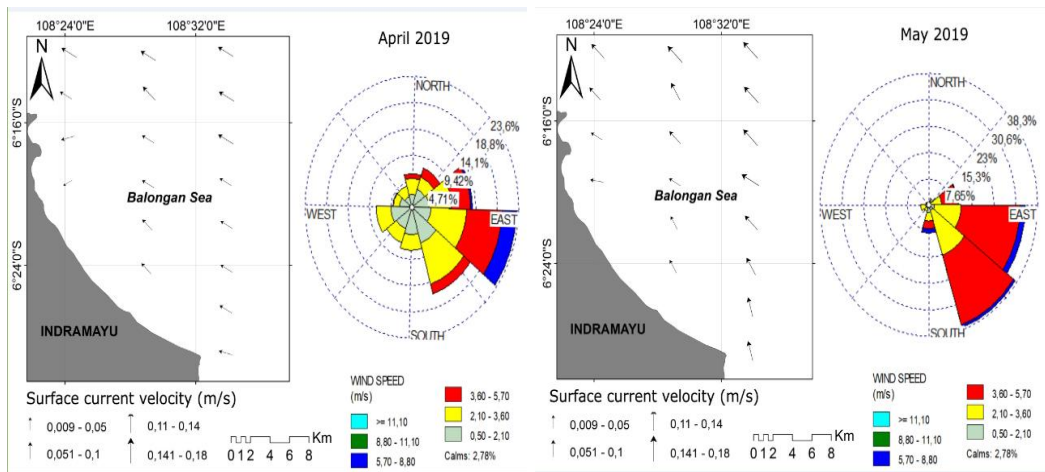


Fig. 6. Sea surface current and wind direction and speed of the transition-1 of April-May 2019.

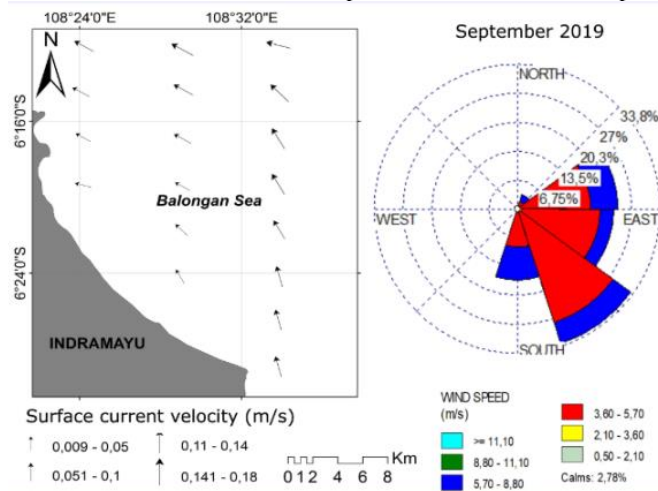


Fig. 7. Sea surface current and wind direction and speed in the east monsoon September 2019.

The result of spatial models for the sea surface current are presented in **Figures 6,7,8 and 9** was developed using data of the physical variables of the seawater such as the average seawater temperature, wind (**Table 4**). The sea surface current in the transition-1 occurred in May 2019 was found as the weakest with $0.038 \text{ m}\cdot\text{s}^{-1}$ current speed and predominantly of northwest direction. The current is lightly increase during the east monsoon of September 2019 and weak again during the transition-2 of October and November 2019. The strongest sea surface current was happened during the west monsoon of February 2020 with current speed of $0.369 \text{ m}\cdot\text{s}^{-1}$ with predominantly southwest direction.

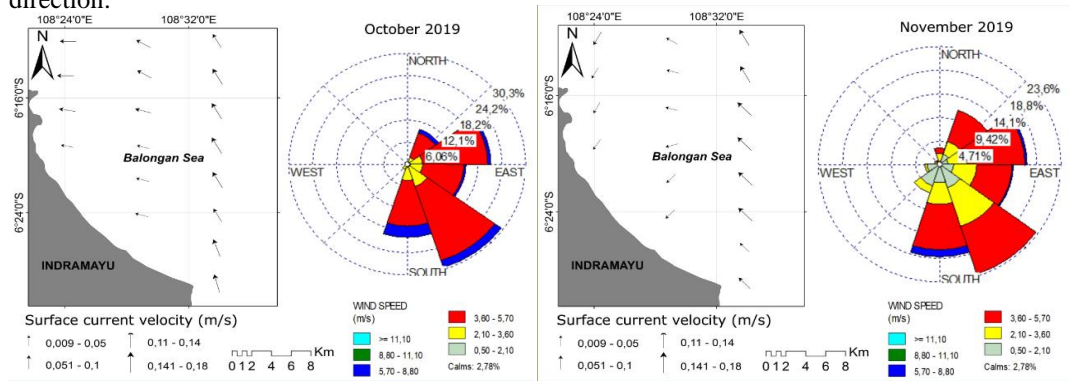


Fig. 8. Sea surface current and wind direction and speed of the transition-2 October-November 2019.

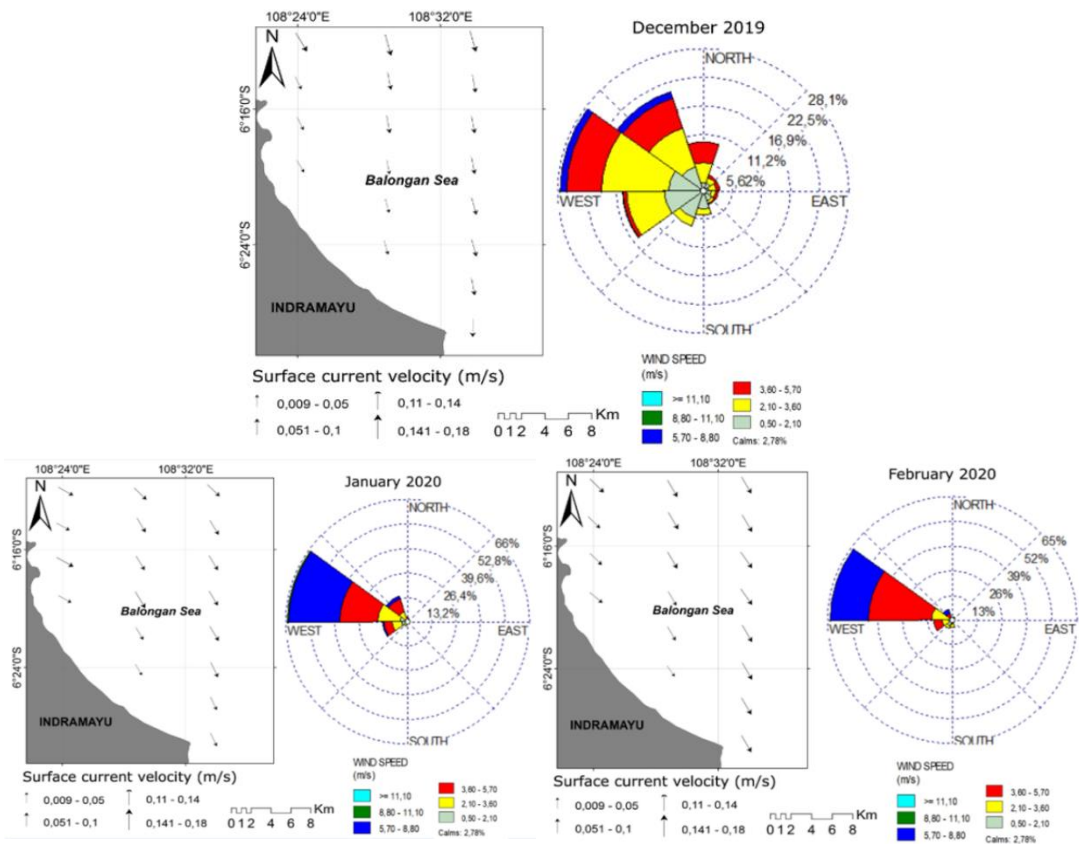


Fig. 9. Sea surface current and wind direction and speed of the west monsoon December 2019 and January – February 2020.

Table 4.

Data of sea surface current and wind direction and speed.

Month	Average Current Speed (m.s ⁻¹)	Average Current Direction	Average Wind Speed (m.s ⁻¹)	Average Wind Direction
April 2019	0.045	Northwest	2.53	West
May 2019	0.038	Northwest	3.28	West
September 2019	0.191	Northwest	4.33	West
October 2019	0.214	Northwest	3.16	West
November 2019	0.139	West	2.51	Southwest
December 2019	0.251	Southeast	2.59	Southeast
January 2020	0.336	Southeast	4.42	East
February 2020	0.369	Southeast	4.19	East

4.3. Oil Spill Spatial Distribution and Trajectory

Result of each of 11 Sentinel-1A SAR data analysis confirmed with oil spill was used as reference to build the trajectory pattern from program running from day-0 to day-10 with input data of wind, sea surface current and tide. Also integrated with the loading and unloading schedule of ships at Balongan coastal water, the type of oil carried by the ships was obtained from PT PERTAMINA Balongan, and produce the trajectory pattern of oil spill using GNOME software. Specifically, the result of spatial distribution, wide area and the trajectory pattern of oil spills were represents type of medium crude oil, light crude oil and diesel oil spill which had indicated to follow the pattern of the sea surface current movement in Balongan coastal water, for four seasons are presented in **Figures 10, 11,12,13** and **Table 4**.

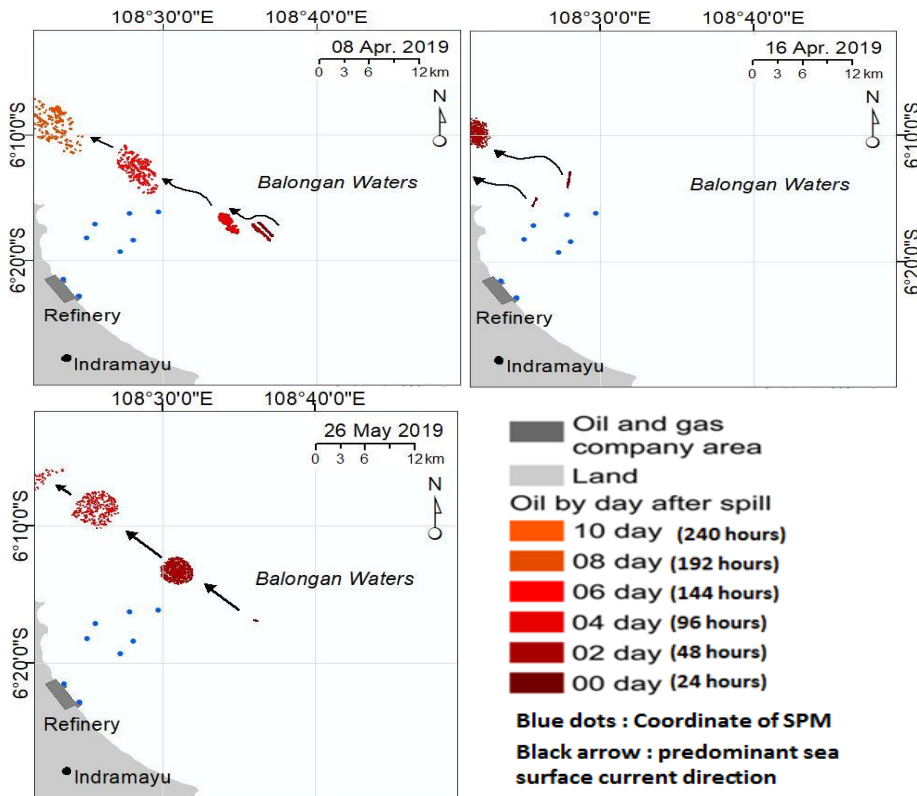


Fig. 10. The northwest oil spill trajectory direction at Balongan coastal water during the transition-1 from April-May 2019. Blue dots are SPM coordinates, red class of oil spill after 10 days trajectory modell.

During the transition-1 period of April-May 2019 (**Fig. 10**) predominant trajectory of oil spill is to the northwest direction from day-0 to day-10. Wide area at day-0 is range of 42.80-113.40 km² and dispersing out of the study area after 240 hours (**Table 5**). Following the east monsoon period (**Fig. 11**) which is only represented in data of September 11, 2019, the spatial trajectory of oil spill pattern to the northwest direction, and wide area of 23.25 km². During the transition-2 in October – November 2019 (**Fig. 12**), oil spill trajectory still with the northwest direction pattern, with wide area of oil spill range 65.54-78.66 km². In the west monsoon period of December 2019, January-February 2020 (**Fig. 13**) oil spill trajectory in contrary to the southeast direction pattern, with wide area range 27.08-107.90 km² (**Table 5**).

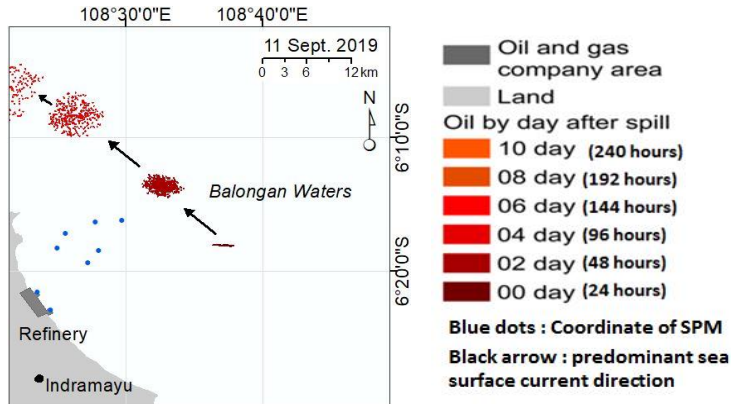


Fig. 11. The northwest oil spill trajectory direction at Balongan coastal water during the east monsoon in September 2019. Blue dots are SPM coordinates, red class of oil spill after 10 days trajectory modell.

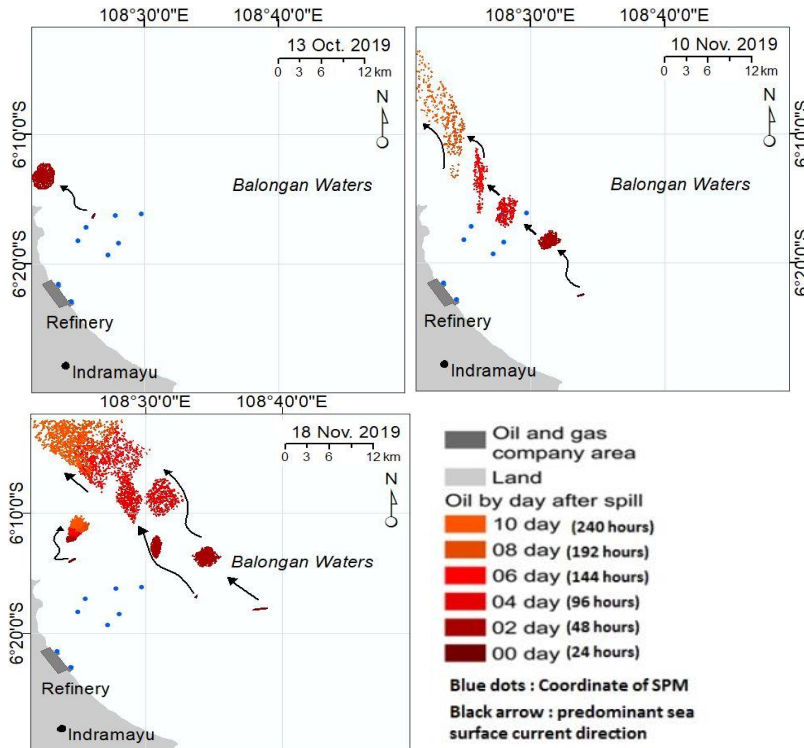


Fig. 12. Predominant northwest oil spill trajectory direction at Balongan coastal water during the transition-2 from October to November 2019. Blue dots are SPM coordinates, red class of oil spill after 10 days trajectory modell.

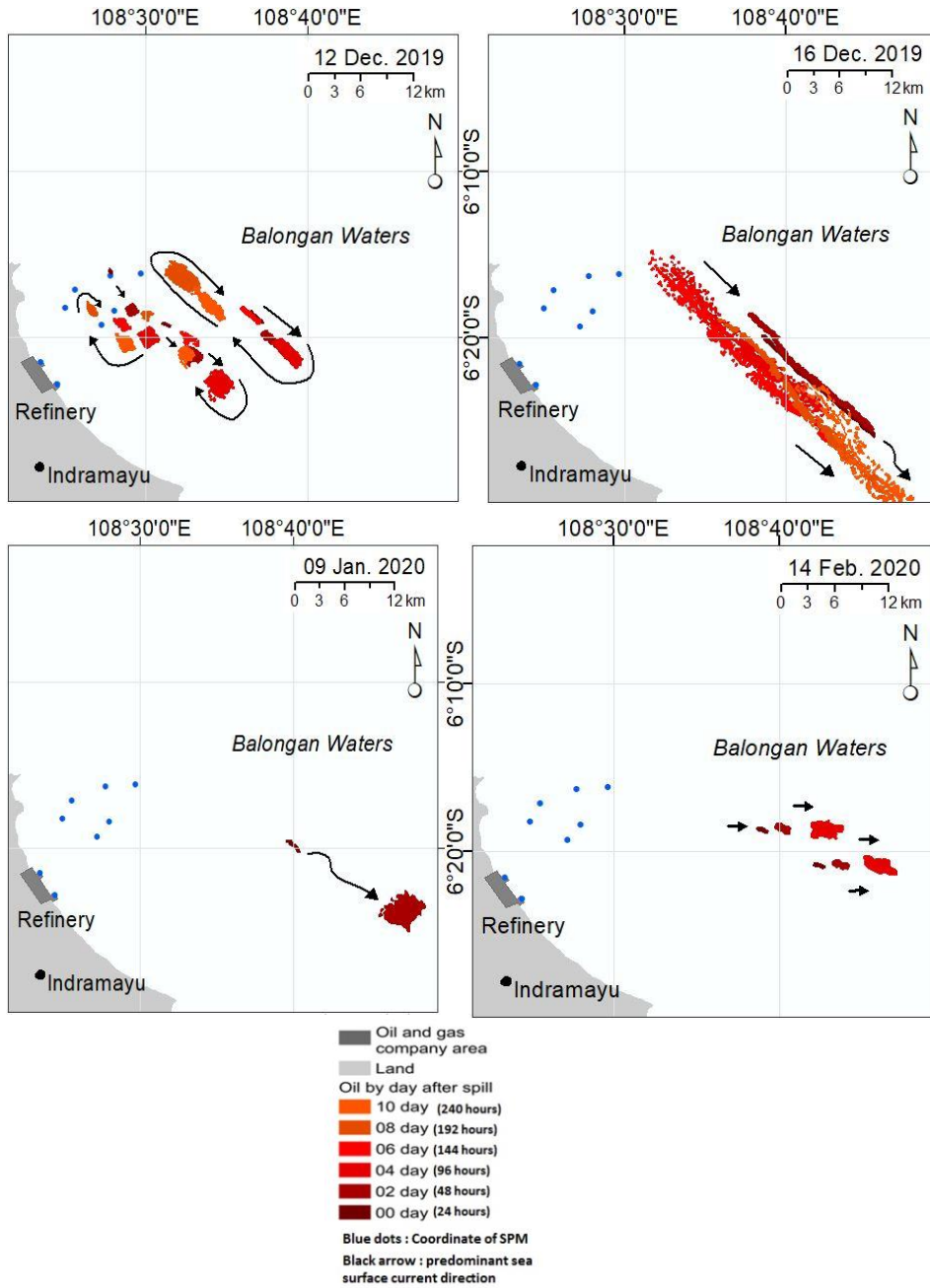


Fig. 13. Predominant southeast trajectory direction of oil spill at Balongan coastal water during the west monsoon from December 2019 to February 2020. Blue dots are SPM coordinates, red class of oil spill after 10 days trajectory modell.

4.4. Oil Spill Volume After Dispersion and Evaporation

The numerical oil trajectory model using GNOME after the evaporation as in **Table 5**.

Table 5.

The wide extent and volume of the oil spill using the GNOME model.

No	Date Detected/ Starting Model	Area Detected (km ²)	Area After 120 hours (km ²)	Area After 240 hours (km ²)	Volume Detected (barrels)	Volume After 120 hours (barrel)	Evaporation after 120 hours (%)
1	08/04/2019	88.30	57.07	-	61.8	33.9	45.1
2	16/04/2019	113.40	-	-	79.3	58.7	26.0
3	26/05/2019	42.80	37.75	-	29.9	20.1	32.5
4	11/09/2019	23.25	25.40	-	11.6	5.0	56.9
5	13/10/2019	78.66	-	-	39.3	21.2	46.1
6	10/11/2019	78.13	37.01	19.98	39.0	20.4	47.7
7	18/11/2019	65.54	16.71	93.54	45.8	24.5	46.5
8	12/12/2019	91.52	12.10	79.90	82.3	64.6	21.5
9	16/12/2019	107.90	14.64	144.85	75.5	41.9	44.5
10	09/01/2020	56.70	-	-	28.3	14.2	49.9
11	14/02/2020	27.08	-	-	13.5	5.9	56.4

Note : the (-) indicate that oil spill had left from the extent of model area.

5. DISCUSSIONS

After four seasonal wind and sea surface current analysis, two predominant wind and sea surface current directions, are east and northeast direction during transition-1 and east monsoon and south to southeast direction during transition-2 and the west monsoon, this in accordance to the study of Alifidini et.al., (2021) as part of regional pattern of Java and Indonesian seas.

Analysis of 58 Sentinel-1A SAR data sets resulted to 11 data sets representing the real field oil spill events for four period from April 2019 to February 2020. Each data was used to build for further oil spill trajectory spatial modell from day-0 to day 10 (240 hours). The oil spill spatial trajectory modell carried out on diesel oil spill had indicated a longer distribution distance compared to the distribution distance of medium crude oil and light crude oil. During the east monsoon condition, in September 11, 2019 and during the transition-2 period of October 13, 2019, type of diesel oil spill of had spreaded to the northwest leaving Balongan coastal water before 240 hours period of the numerical model run. This has showed that the light density of diesel oil was very easy to flows in accordance to the sea surface currents and also easily evaporates. Similar to what happened in the west monsoon, diesel oil spill the during period of January 9 and February 14, 2020 was also very quickly left Balongan coastal water towards the southeast direction before the numerical model had been ranned for 120 hours period. During the east monsoon, the light crude oil spill for the period of April 8 and 16, and May 26, 2019, after the numerical modell ranned for 240 hours, had shown the oil spills spread out from Balongan coastal water to the northwest direction. During the west monsoon, the light crude oil spill had moved to the southeast direction in the period of October 18 and December 16, 2019. This was in accordance with the movement of the sea surface currents that flows to the northwest and southeast according to the monsoon. Likewise, the medium crude oil spill which has a higher oil density than diesel and light crude oil, had moved in the same direction as the direction of the sea surface current, but with slower movement and distribution than the other two types of oil spill.

Oil spill spatial trajectory analysis using GNOME method, revealed that the period of the oil spills detected were happened almost evenly distributed at every month, which the oil spill area extent found in the range of 23.25 – 113.40 km². Lowest area of oil spill of 23.25 km² in September, 11.2019 was in accordance with smallest oil spill volume of 11.6 barrels (Table 5). The widest area of oil spill of 113.40 km² in April, 16.2019 was assumed related to the volume of oil spill detected of 79.3 barrels. Specific condition of the biggest volume of oil spill 82.3 barrels occurred in December 12, 2019 and was assumed related to the rough wave at the SPM condition during loading and unloading process. Very interesting finding of the lowest evaporation rate of 21.5% in this month is in fact happened

during the west monsoon or the peak of the rainy season. While the highest evaporation rate of 56.9% found in the model in September, 11 2019 (Table 5) which is related to the condition of higher sea surface and atmospheric air temperature during the peak of the east monsoon or the dry season.

Specific finding also which oil spills in April 4, 2019 with 88.30 km² initial wide area in day-0 had experienced a significant decrease to 57.07 km² wide area after 120 hours trajectory model, and then dispersed finely to zero after the period of 240 hours trajectory model. In contrast, in data of December 16, 2019 that initial oil spill wide area of 107.90 km² in day-0 then decrease to 14.74 km² after 120 hours trajectory model, but then increase significantly to become 144.85 km² after 240 hours (Table 5), which is refer to the rough wave and sea surface current (Figure 9) during the west monsoon. After 120 hours of moving in the sea water, and the evaporation rate of oil spill range is between 26 – 56.9%. The numerical spatial model had shown a relatively high evaporation rate of oil spills after 240 hours period. Initial process of the oil spill enters the marine environment, the oil spill will undergo a spreading process. Which this initial process is the most important process during the initial and trajectory of oil spill into the marine environment. The entry of oil spill into the marine environment will be followed by various processes that will occur and effected by the physical conditions of the waters, one of which is sea surface currents. According to Zhang *et al.* (2019) that the spread and volume of oil spill on the sea will be primarily affected by the sea surface currents.

Naz *et al.* (2021) observed four oil spill events in the Indian Ocean including Chennai, Sharjah, Al Khiran and Mubarak Village analyzed using Sentinel-1 SAR data. The GNOME model was used for the production of the oil spill trajectory, while the oil spill weathering process was modeled using the Automated Data Inquiry for Oil Spill (ADIOS). The maximum oil spill movement (33 km) from the source point was observed at Al Khiran, while the rate of evaporation of crude oil was observed to be high. Balogun *et al.* (2021) developed an oil spill environmental vulnerability model to predict and map the trajectory of an oil spill in Kota Tinggi, Malaysia. Oil spill scenarios were being simulated using the GNOME. The results showed that the oil layer velocity at 40.8 m per minute was higher during the pre-monsoon period in the southwest and lower during the northeast monsoon (36.9 m per minute).

The high evaporation rate of oil spills had been generated in this research model was similar value to the evaporation of oil spills produced by Toz, (2017) in Samsun Bay Turkey and Afenyo *et al.*, (2016) in the Arctic Sea, and Ramirez *et al.*, (2019) in the Caribbean Sea, Colombia. This evaporation process had caused the volume of the oil spill to be reduced by an average of 43%. As in Table 5 showed that the volume of detected oil spills decreased by an average of 17.81 barrels after 10 hours. In the period during April 16 and October 13, 2019, the oil spill had moved outside the model limits after 120 hours as well as after 240 hours. This was because the occurrence of oil spills was generally located in the western part of the study area. Also when the model was ran for more than 120 hours during the east monsoon, it would be out of model limit area. Meanwhile, during the west monsoon, the average of oil spill area was spread evenly over the study area, mean that the volume of oil spill could still be analyzed within the model limits. The trajectory model showed that oil spills that occur during the period of the study in one year in the limit of the study area did not reach to the coast due to the effect of sea surface current and wind of northwest and southeast direction pattern. Oil spills direction pattern was mainly driven by sea surface currents moved parallel along to the coastline direction and away from the coastline, so that within the model limits during the study there were no oil spills that have been detected to reach and pollution to the coastline area. Difference with the current study in this research with the case that oil spill occurred on the sea surface caused by floating infrastructure of SPM. Another study by Heidaria *et al.* (2019), as comparison which had examined a more advanced modelling for assessing spatial and stochastic oil spill risk, which is a very specific case study of an oil spill from a sunken ship in Kattegat located between Denmark and Sweden in Northern Europe's inlet to the Baltic Sea. They use the VRAKA method which was used to estimate the probability of release in a quantitative oil spill risk assessment and 3D plumes using the GNOME. This research demonstrated the spatial and stochastic risk assessment of oil spills from shipwrecks, allowing a structured approach to incorporate the complex factors that influence the risk values.

6. CONCLUSIONS

Spatial modelling of wind and sea surface current, in general exhibit a predominant wind and sea surface current during transition-1 April-May until the east monsoon of September 2019 is the east direction. Predominant wind and sea surface current during transition-2 of October-November 2019 and during the west monsoon of December 2019-February 2020 is south and southeast direction, parallel to the coastline morphology.

Analysis of oil spills using 58 Sentinel-1A SAR data had confirmed 11 data on April 8 and 16, May 26 representing for the transition-1 period, only one oil spill event in September 11 to represents for the east monsoon. SAR data in October 13, and November 10 and 18, 2019 had confirmed the event of oil spill to represent for transition-2 period. SAR data in December 12 and 16, 2019, January 09, and February 14, 2020 to represents for the west monsoon with predominant to the southeast direction. The study had revealed that oil spills had moved mainly in accordance to sea surface current and seasonal wind direction based on the wind rose data. In the east monsoon, the wind and currents were generally dominated to the west and northwest from the east. Meanwhile, during the west monsoon, the wind and current directions from the west to the southeast and east.

The most important and critical finding based on integration of spatial Sentinel-1A SAR data, GNOME hydrodynamic- trajectory modelling revealed the oil spill trajectory, wide area, type, volume and evaporation rate of the oil spill. The smallest area of oil spill is 27.08 km² in the east monsoon of February 2020 and widest area of 113.40 during the transition-1 of April 2019 and widest area become 144.85 km² after 240 hours period during the west monsoon of December 16.2019. Total detected oil spill volume of 773.28 barrels with an evaporation rate of 43% after 120 hours of numerical modelling, with average of 70.30 km² of oil spill area. The trajectory direction of the oil spill in the east monsoon was spread toward the northwest of Balongan coastal water, while during the west monsoon the spill moved toward the southeast. Smallest oil spill volume 11.6 barrel had been detected but with highest evaporation rate of 56.9% occurred in September 2019 of the east monsoon. Biggest volume of oil spill of 82.3 barrel occurred in December 2019 west monsoon with lowest evaporation rate of 21.5%.

ACKNOWLEDGEMENT

The authors would like to thanks especially to the Institute for Research and Community Development – Diponegoro University for the funding support in contract no. 233-39/UN7.6.1/PP/2021 and other parties for their help and guide to the manuscript. Also to the Faculty of Fisheries and Marine of Universitas Diponegoro. University for the research funding No:19/UN7.5.10/PP/2019 APBN.FPIK Undip TA 2019.

REFERENCES

- Afenyo, M., F. Khan, B. Veitch, dan M. Yang. (2016). Modeling Oil Weathering and Transport in Sea Ice. *Marine Pollution Bulletin*, 107(1): 206–215.
- Alifidini, I., Shimada, A., Wirasatriya. 2021. Seasonal Distribution and Variability of Surface Winds in the Indonesian Seas Using Scatterometer and Reanalysis Data. *International Journal of Climatology*. <https://doi.org/10.1002/joc.7101>
- Balogun, A. L., S. T. Yekeen., B. Pradha., K. B. W. Yusof. 2021. Oil spill trajectory modelling and environmental vulnerability mapping using GNOME model and GIS. *Environmental Pollution*. 268 : 115812.
- Cantorna, D., C. Dafonte., A. Iglesias., B. Arcay. 2019. Oil spill segmentation in SAR images using convolutional neural networks. A comparative analysis with clustering and logistic regression algorithms. *Applied Soft Computing Journal*. 84 : 105716.
- Chaturvedi, S. K., S. Banerjee., S. Lele. 2020. An assessment of oil spill detection using Sentinel 1 SAR-C images. *Journal of Ocean Engineering and Science*. 5 : 116–135.
- Fan, J., F. Zhang, D. Zhao, dan J. Wang. 2015. Oil Spill Monitoring Based on SAR Remote Sensing Imagery. *Aquatic Procedia*, 3: 112–118.

- Fitriyanto, B. R., M. Helmi, and Hadiyanto. 2019. Analyzing Spatiotemporal Types and Patterns of Urban Growth in Watersheds that Flow into Jakarta Bay, Indonesia. *Remote Sensing Applications: Society and Environment*, 14: 170 - 177.
- Fletcher, K., 2012. Sentinel-1: ESA's Radar Observatory Mission for GMES Operational Services. ESA Communications, SP-1322/1.
- Hartoko, Agus, Muhamad Helmi, Mujahid Sukarno, Hariyadi. 2016. Spatial Tsunami Wave Modelling for the South Java Coastal Area, Indonesia. *International Journal of Geomate*. Vol 11 (25) : 2455-2460.
- Hartoko Agus, Arief Febrianto, Aditya Pamungkas, Irvani Fachruddin, Muhammad Helmi, Hariyadi. 2019. The Myth and Legend of Sadai and Gaspar Strait Bangka Belitung (BANCA-BILLITON) and Oceanographic Conditions. *International Journal of Geomate*. 62 : 212-218. <https://doi.org/10.21660/2019.62.93965>.
- Heidari, P. A., L. Arneborg, J. F. Lindgren, A. Lindhe, L. Rosén, M. Raie, L. Axell, dan I. M. Hassellöv. 2019. A State of the Art Model for Spatial and Stochastic Oil Spill Risk Assessment: A Case Study of Oil Spill from a Shipwreck. *Environment International*, 126: 309–320.
<https://www.ecmwf.int>
<https://www.hycom.org>
<https://scihub.copernicus.eu>
- Josaphat, T. S. S and N. Imura. 2016. Development of Curcularly Polarized Synthetic Aperture Radar for Aircraft and Microsatellite. *IEEE International Geoscience and Remote Sensing Symposium (IGARSS)*. 5654 – 5657.
- Kingston, P. F. 2002. Long-term Environmental Impact of Oil Spills. *Spill Science & Technology Bulletin*, 7(1-2): 53-61.
- Lehr, W., R. Jones, M. Evans, D. Simecek-Beatty, dan R. Overstreet. 2002. Revisions of the ADIOS Oil Spill Model. *Environmental Modelling & Software*, 17(2): 189–197.
- Li, G., Y. Liu, P. Wu, & C. Chen. 2019. Marine Oil Slick Detection Based on Multi-Polarimetric Features Matching Method Using Polarimetric Synthetic Aperture Radar Data. *Sensors*, 19: 5176 p.
- Liu, X., J. Guo, M. Guo., X. Hua., C. Tang., C. Wang., Q. Xing. 2015. Modelling of oil spill trajectory for 2011 Penglai 19-3 coastal drilling field, China. *Applied Mathematical Modelling*. 39 : 5331–5340.
- Mera, David., Cotos, J.M., Varela-Pet, J & Garcia-Pineda, Oscar. 2012. Adaptive Thresholding Algorithm Based on SAR Images and Wind Data to Segment Oil Spills along The Northwest Coast of The Iberian Peninsula. *Marine Pollution Bulletin*, 64:2090 – 2096.
- Naz, S., M. F. Iqbal., I. Mahmood., M. Allam. 2021. Marine oil spill detection using Synthetic Aperture Radar over Indian Ocean. *Marine Pollution Bulletin*. 162 : 111921.
- Nordam T., CJ. Beegle-Krause., J. Skancke., R. Nepstad., M. Reed. 2019. Improving oil spill trajectory modelling in the Arctic. *Marine Pollution Bulletin*. 140 : 65–74.
- Qiao, f., G. Wang., L. Yina., K. Zeng., Y. Zhang., M. Zhang., B. Xiao., S. Jiang., H. Chen., G. Chen. 2019. Modelling oil trajectories and potentially contaminated areas from the Sanchi oil spill. *Science of the Total Environment*. 685 : 856–866.
- Rajendran, S., P. Vethamony., F. N. Sadooni., H. A. S. Al-Kuwari., J. A. Al-Khayat., H. Govil., S. Nasir. 2021. Sentinel-2 image transformation methods for mapping oil spill –A case study with Wakashio oil spill in the Indian Ocean, off Mauritius. *MethodsX*. 8 : 101327.
- Ramírez, J., A. Merlano, J. Lacayo, A. F. Osorio, dan A. Molina. 2017. A Model for the Weathering of Colombian Crude Oils in the Colombian Caribbean Sea. *Marine Pollution Bulletin*, 125(1-2): 367–377.
- Remyalekshmi, R dan A. V. Hedge. 2013. Numerical Modeling of Oil Spill Movement along North-West Coast of India Using GNOME. *International Journal of Ocean and Climate System*., 4(1): 75-86.
- Sauz, F. G. R., T. F. Reyes, C. Costa. 2018. Laser Induced Breakdown Spectroscopy (LIBS) for Express Identification of Crude Oils. *Revista Cubana De Física*, vol 35(1): 19-23.
- Sinurat, M.E.Br., A. Ismanto, and Hariyadi. 2016. Analysis of Crude Oil Spill Spatial Pattern Using Hydrodynamic Model at Balongan, Indramayu, Java Sea. *Jurnal Oseanografi UNDIP*, 5(2):218 - 226.
- Sun, S., C. Hu, L. Feng, G. A. Swayze, J. Holmes, G. Graettinger, I. MacDonald, O. Garcia, and I. Leifer. 2016. Oil Slick Morphology Derived from AVIRIS Measurements of the Deepwater Horizon Oil Spill: Implications for Spatial Resolution Requirements of Remote Sensors. *Marine Pollution Bulletin*, 103(1-2): 276–285.
- Susanti, Y., S. Syafrudin, and M. Helmi. 2019. Soil Erosion Modelling at Watershed Level in Indonesia: a Review. *E3S Web of Conferences, ICENIS 2019*, 125: 01008.
- Toz, A. C. 2017. Modelling Oil Spill around Bay of Samsun, Turkey, with the Use of Oilmap and Adios Software Systems. *Polish Maritime Research*, 24(3): 115–125.

- Wirasatriya, A., H. Kawamura, M. Helmi, D. N. Sugianto, T. Shimada, K. Hosoda, G. Handoyo, Y. D. G. Putra, dan M. Koch. 2020. Thermal Structure of Hot Events and Their Possible Role in Maintaining the Warm Isothermal Layer in the Western Pacific Warm Pool. *Ocean Dynamics*, 70: 771 - 786.
- Yang, Y., Z. Chen., Y. Li., X. Xiao., Q. Dan., T. Yang dan Z. Ren. 2013. Numerical Simulation of Oil Spill in The Gulf of Mexico Based on GNOME and ADIOS. *Journal Applied Mechanics and Materials* Vols. 295-298.
- Yu, X., W. Zhang, X. Liu, J. Lei, Z. Lin, Z. Yao, X. Yao, X. Jin, H. Yang, H. Huang. 2018. The Distribution of and Biodegradation Impact on Spilled Oil in Sediments from Dalian Bay, NE China. *Marine Pollution*, 135: 1007–1015.
- Zhang, B., E. J. Matchinski, B. Chen, X. Ye, L. Jing, dan K. Lee. 2019. Marine Oil Spills - Oil Pollution, Sources and Effects. *World Seas: An Environmental Evaluation*, 21: 391–406.